Rhinovirus Induces Airway Epithelial Gene Expression through Double-Stranded RNA and IFN-Dependent Pathways

Yin Chen, Edward Hamati, Pak-Kei Lee, Wai-Ming Lee, Shinichiro Wachi, David Schnurr, Shigeo Yagi, Gregory Dolganov, Homer Boushey, Pedro Avila, and Reen Wu

University of California at Davis, Davis; California Department of Health Services, Richmond; University of California at San Francisco, San Francisco, California; and University of Wisconsin, Madison, Wisconsin

Rhinovirus (RV) infection is the major cause of common colds and of asthma exacerbations. Because the epithelial cell layer is the primary target of RV infection, we hypothesize that RV-induced airway disease is associated with the perturbation of airway epithelial gene expression. In this study, well differentiated primary human airway epithelial cells were infected with either RV16 (major group) or RV1B (minor group). Transcriptional gene profiles from RV-infected and mock-infected control cells were analyzed by Affymetrix Genechip, and changes of the gene expression were confirmed by real-time RT-PCR analysis. At 24 h after infection, 48 genes induced by both viruses were identified. Most of these genes are related to the IFN pathway, and have been documented to have antiviral functions. Indeed, a significant stimulation of IFN-β secretion was detected after RV16 infection. Neutralizing antibody specific to IFN-β and a specific inhibitor of the Janus kinase pathway both significantly blocked the induction of RV-inducible genes. Further studies demonstrated that 2-aminopurine, a specific inhibitor double-stranded RNA–dependent protein kinase, could block both IFN-β production and RV-induced gene expression. Thus, IFN-β–dependent pathway is a part of the double-stranded RNA–initiated pathway that is responsible for RV-induced gene expression. Consistent with its indispensable role in the induction of antiviral genes, deactivation of this signaling pathway significantly enhanced viral production. Because increase of viral yield is associated with the severity of RV-induced airway illness, the discovery of an epithelial antiviral signaling pathway in this study will contribute to our understanding of the pathogenesis of RV-induced colds and asthma exacerbations.

Keywords: airway epithelium; gene expression; rhinovirus; transcriptional profiling

Rhinovirus (RV) is a small (30 nm in diameter), nonenveloped, positive-stranded RNA virus (1). More than 100 serotypes have currently been identified. Except for RV87 (an enterovirus misidentified as RV), all the serotypes can be divided into major or minor groups based on their specific interactions with the cellular receptors: intercellular adhesion molecule 1, which is the receptor for the major group; or a member of the low-density lipoprotein receptor family, which is the receptor for the minor group (1).

RV infection causes at least half of all common colds each year (2). In addition to causing the typical symptoms of rhinitis, sinusitis, and middle-ear dysfunction, RV infection can also cause lower respiratory complications, such as wheezing, small-airway obstruction, bronchitis, bronchiolitis, and pneumonia, especially in susceptible populations (3). In children or adults with asthma, RV infection is commonly associated with exacerbations of the condition (4). Using a sensitive PCR assay along with traditional viral detection techniques, Johnston and colleagues found that 80–85% of school-aged children with wheezing episodes tested positive for a virus. In most cases, the virus identified was RV (5). This was also found to be true of asthma exacerbation in adults; approximately half are found to be associated with RV infection (6). Moreover, it appears that the seasonal patterns of viral respiratory infection correlate closely with hospital admissions for asthma, especially in children (7), which further indicates the severity of virus-induced asthma. Taken together, these studies indicate that viral infections, particularly RV infection, are the most common cause of asthma exacerbations and contribute to the morbidity of asthma in both children and adults.

The site of RV infection is airway epithelial cells. RV can enter other airway cell types, such as monocyte and macrophage, but does not replicate in these cells (8), which further emphasizes the importance of epithelial cells in initiating the host response to viral infection. In addition, several recent studies have demonstrated that RV infection and viral replication can occur in the lower as well as upper airways (9–11). Given the close association between the worsened inflammation of the lower airways and worsening of asthma, RV infection of the lower airway epithelium may be more relevant to the asthma exacerbations.

Although the relationship between RV infection and asthma exacerbation has been well established by clinical epidemiologic studies, the molecular mechanisms by which RV infection triggers the inflammatory response are poorly understood. Several recent studies have demonstrated significant elevation of cytokine gene expression (*IL-1*, *IL-6*, *IL-8*, *GM-CSF*, *eotaxin, RANTES*) (12–15) by epithelial cells after RV infection. Thus, those inflammatory mediators may enhance airway inflammation and trigger airway disease exacerbations. In addition, early studies (16, 17) indicated a direct correlation between titer of secreted virus and occurrence, as well as severity of illness. Most recently, Wark and colleagues have demonstrated that RV-infected asthmatic airway epithelial cells produced much more virus than normal cells, which was caused by the deficiency of epithelial antiviral response in asthmatic cells (18). Thus, a significant increase in viral production under diseased condition may also contribute to RV-induced airway disease exacerbations.

To examine the primary, direct airway epithelial response to RV infection, we performed unbiased gene profiling using Affymetrix Genechip (Affymetrix, Inc., Santa Clara, CA) in well differentiated polarized, primary human TBE cells. Using this approach, we have identified novel RV-induced epithelial genes, most of which are related to the IFN pathway and have antiviral

(*Received in original form December 28, 2004 and in final form September 20, 2005*)

The study was supported by grants from the California Tobacco-Related Disease Research Program (13KT-0101) and from the National Institutes of Health (NIH) (DE015845) to Y.C. and (AI50496, HL35635, HL077315, HL007013) to R.W.

Correspondence and requests for reprints should be addressed to Yin Chen, Ph.D., Center for Comparative Respiratory Biology and Medicine, Genomic and Biomedical Sciences Facility, Suite 6510, University of California at Davis, One Shields Ave., Davis, CA 95616. E-mail: yinchen@ucdavis.edu

Am J Respir Cell Mol Biol Vol 34. pp 192–203, 2006
Originally Published in Press as DOI: 10.1165/rcmb.2004-0417OC on October 6, 2005
Internet address: www.atsjournals.org

functions. Our analysis of the underlying molecular mechanism has revealed two pathways for RV-induced epithelial gene expression: a double-stranded RNA (dsRNA)–dependent protein kinase (PKR) signaling pathway, and a PKR-induced IFN-β autocrine/paracrine pathway. Deactivation of these pathways significantly enhanced viral production, which further emphasizes their indispensable role in epithelial antiviral response.

MATERIALS AND METHODS

RV, Inhibitors, and Antibodies

RV16 and RV1B stocks were amplified and purified based on the previous published protocol (19). Briefly, HeLa cell suspension was infected at room temperature for 1 h with a multiplicity of infection (MOI) of 10–15 PFU per cell. Infected cell suspensions were diluted 10-fold in prewarmed medium B and incubated at 35°C for 7–8 h. The cells were then pelleted and resuspended in PBS. Virus was released from cells by three cycles of freezing and thawing and then harvested as the supernatant after centrifugation to pellet cell debris. Sucrose gradient was used to purify the virus particles released from cells. Viral titers were determined by plaque assay as described previously (19). Anti-RV16 monoclonal antibody was a gift from Dr. James E. Gern (University of Wisconsin, Madison). Chemical inhibitors (2-aminopurine [2-AP] and Janus kinase [JAK] inhibitor I) were purchased from Calbiochem (EMD Biosciences, Inc., San Diego, CA). Neutralizing antibody (anti–IFN-β) was purchased from R&D Systems Inc. (Minneapolis, MN). To make replication-deficient RV16 (UV-RV16), stocks of RV16 were ultraviolet irradiated, as described previously (20), with a slight modification. Briefly, 1 ml RV stock solution, containing 5×10^8 RV16, was exposed to 200 μW cm^{-2} ultraviolet light for 10 min on ice.

Cell Culture Condition for Primary Airway Epithelial Cells and Viral Infection

Human tracheobronchial tissues were obtained from National Disease Research Interchange, with an approved protocol. The University of California, Davis Human Subjects Review Committee approved all procedures involved in tissue procurement. We have, in the past, successfully established primary airway epithelial cultures from these tissues (21). Normally, primary cells were plated on a Transwell (Corning Costar, Corning, NY) chamber (25 mm) at $1–2 \times 10^4$ cells/cm^2, in a Ham's F12:Dulbecco's modified Eagle's medium (1:1) supplemented with eight factors, including: insulin (5 μg/ml), transferrin (5 μg/ml), epidermal growth factor (10 ng/ml), dexamethasone (0.1 μM), cholera toxin (10 ng/ml), bovine hypothalamus extract (15 μg/ml), BSA (0.5 mg/ml), and all-*trans*-retinoic acid (30 nM). After a week in immersed culture condition, cultured cells were shifted to an air–liquid interface culture condition. Under the biphasic culture condition, high transepithelial resistance ($> 500\ \Omega \cdot cm^2$), cilia beating, and the formation of mucus-secreting granules were observed (22). Normally, experiments were performed at Day 21 or 2 wk after the change of the culture condition from immersed to air–liquid interface. Medium was routinely changed once every other day. Immediately before RV inoculation, cells were grown overnight (16 h) in media with only BSA and all-*trans*-retinoic acid. Subsequent RV infection was also performed using media containing these two factors.

Infection was performed based on the protocol described previously (23). Briefly, to mimic *in vivo* RV infection, 200 μl of media containing the specific concentration (as indicated in the text) of live virus was added onto the apical side of the cells for the desired time period, as described in the text. Because the viral particles were purified and suspended in PBS, the same volume of PBS was used for the mock-infected control. Before the collection of cellular RNA and protein, the cell surface was washed three times with PBS to ensure removal of all nonattached viral particles. The lack of remaining inoculum was confirmed by PCR assay of the final wash.

A 50% tissue culture infective dose ($TCID_{50}$) assay (11) was used to measure extracellular viral yield. Briefly, cells were infected with RV for 24 h. Cell surface was then completely washed and replaced with fresh medium. After 24 h, viral yields in both apical and basal media were determined.

Toxicity Measurement on Viral Infection and Chemical Inhibitor Treatment

Light microscopy and lactate dehydrogenase (LDH) assay were used to monitor the potential toxicity caused by viral infection and chemical inhibitor treatment. Dead and "sloughed-off" cells were obvious in RV-infected culture after 24 h, but not in the culture treated with 2-AP or JAK inhibitor 1 only. LDH assay kit (Promega, Inc., Madison, WI) was used, based on the manufacturer's instructions, to measure cellular toxicity by determining LDH release from damaged cells. Briefly, to determine LDH activity, after removal of the medium, the cells were lysed using a lysis buffer (LDH assay kit), centrifuged at $16{,}000 \times g$ for 1 min, and the supernatants assayed for LDH activity. This cell-associated LDH activity was then added to the LDH activity in the removed culture medium, and the total activity was considered to represent 100% cell death. The amount of LDH present in the medium was then calculated as a percentage of the total, which determined the percent cell death in that sample (data was shown).

Transcriptional Gene Profiling by Affymetrix Genechip

The HGU133A chip that contains 22,283 probe set was used, and all protocols used in this study were based on the manufacturer's instruction (Affymetrix, Inc.). The double-extracted total RNA was submitted to the core microarray facility of the University of California, Davis, Cancer Center. At this facility, RNA samples were prepared, hybridized to these array chips, and the hybridization signals were scanned using the standard protocols suggested by Affymetrix. For quality control, the scanned images of each array were visually inspected to be free of artifacts. Scatter plots of individual arrays were also used to assess the overall quality of the array data.

Affymetrix HGU133A oligonucleotide microarray was used for the experiment. Bioconductor, a biological data analysis package based on R statistical programming language (Vienna University of Technology; http://www.r-project.org/), was used for array data analysis and integration with other gene annotations. Normalization algorithms used were robust multichip average (24). Robust multichip average–derived expression values were used for the rest of the analysis. An expression level of over 2-fold average difference was required for a candidate gene to qualify as a differentially expressed gene of relevance to our study. Two-fold difference is an arbitrary but well accepted threshold of biologically relevant differential gene expression. The Genechip assay was repeated on two separate cultures derived from two normal

TABLE 1. REAL-TIME POLYMERASE CHAIN REACTION PRIMERS

Gene	Primers
RV16	Forward: TCTCTACAGGGCCCTTACTCG
	Reverse: CCACTCTTCTCTCGGGAACTT
RV1B	Forward: CCATCGCTCACTATTCAGCAC
	Reverse: TCTATCCCGAACACACTGTCC
CXCL10	Forward: CCTTAAAACCAGAGGGGAGC
	Reverse: CCTCTGTGTGGTCCATCCTT
BST2	Forward: AAGAAAGTGGAGGAGCTTGAGG
	Reverse: CCTGGTTTTCTCTTCTCAGTCG
ISG15	Forward: GGACCTGACGGTGAAGATGCT
	Reverse: ACGCCAATCTTCTGGGTGATCT
RIG1	Forward: CTTGGCATGTTACACAGCTGAC
	Reverse: GCTTGGGATGTGGTCTACTCA
STAT1A	Forward: TCAGACCACAGACAACCTGC
	Reverse: AGAGCCCACTATCCGAGACA
IRF7	Forward: GTGTGTCTTCCCTGGATAGCAG
	Reverse: CCATAAGGAAGCACTCGATGTC
LAMP3	Forward: AGTGAACAGAGCCTCCAGTTGT
	Reverse: TAGTCAGACGAGCACTCATCCA
Mx1	Forward: AGAGAAGGTGAGAAGCTGATCC
	Reverse: TTCTTCCAGCTCCTTCTCTCTG
OAS1	Forward: GCTCCTACCCTGTGTGTGTGT
	Reverse: TGGTGAGAGGACTGAGGAAGA
GAPDH	Forward: CAATGACCCCTTCATTGACC
	Reverse: GACAAGCTTCCCGTTCTCAG

individuals. Only those genes that showed significant changes in both experiments were subject to the further study.

Real-Time RT-PCR

Real-time PCR was performed as described previously (25). cDNA was prepared from 3 μg of total RNA with Moloney murine leukemia virus (MoMLV)–reverse transcriptase (Promega, Inc.) by oligo-dT primers for 90 min at 42°C in a 20-μl reaction solution, and was then further diluted to 100 μl with water for the following procedures. Two microliters of diluted cDNA was analyzed using 2× SYBR Green PCR Master Mix by an ABI 5700 or ABI Prism 7900HT Sequence Detection System (Applied Biosystems Inc., Foster City, CA), following the manufacturer's protocol. Primers are listed in Table 1, and were used at 0.2 μM. The PCR reaction was performed in 96-well optical reaction plates, and each well contained a 50-μl reaction mixture. The SYBR green dye was measured at 530 nm during the extension phase. The relative mRNA amount in each sample was calculated based on the $\Delta\Delta C_t$ method using housekeeping gene *GAPDH*. The purity of amplified product was determined from a single peak of a dissociation curve. Efficiency curves were performed for each gene of interest relative to the housekeeping gene, based on the manufacturer's instructions. Real-time PCR was generally repeated six times on the primary TBE cultures derived from a minimum of two different donors. Results were calculated as fold induction over control, as described previously (25).

Western Blot

Total cellular protein was collected based on the methods described previously (26). Anti–phospho–signal transducer and activator of transcription (STAT) 1, anti-STAT1, anti–phospho-PKR antibodies (Cell Signaling Technology, Inc., Beverly, MA) were used in the Western blot analysis as described previously (26). Equal protein loading was confirmed using the staining of anti–β-tubulin antibody (Sigma-Aldrich Corp., St. Louis, MO).

ELISA Assay

Human IFN-α, IFN-γ Quantikine ELISA kit (R&D Systems Inc., Minneapolis, MN), and IFN-β ELISA kit (Biosource International, Camarillo, CA) were used to measure the secreted IFN concentrations in the media, following the manufacturer's instructions.

Statistical Analysis

Experimental groups were compared using a two-sided Student's *t* test, with significance level set as $P < 0.05$. When data were not distributed normally, significance was assessed with the Wilcoxon matched-pairs signed-ranks test, and $P < 0.05$ was considered to be significant. Matlab 6.0 with statistics toolbox (MathWorks, Inc., Natick, MA) was used for analyses of the data.

RESULTS

Time-Dependent RV Replication in Polarized Primary TBE Cells

The primary target of RV infection is the luminal side of the airway epithelia. To mimic *in vivo* RV infection on airway epithelial cells, well differentiated human primary TBE cells were apically infected with RV 16 (a representative of the major group of RV) and RV1B (a representative of the minor group of RV) at 10^7/ml PFU, respectively. This dose is equivalent to an MOI of 10. In a previous study, we found that the peak viral titer in the nasal washings obtained after RV-induced cold in human volunteers was $\sim 10^6$ viral particle/ml by multiplying the dilution factor (P. Avila and S. Yagi, personal communication). Considering the incompleteness of the washing protocol, we estimated 10^7 PFU/ml as an appropriate infection dose.

Using this infection protocol, we performed time-course analyses of viral replication in primary human TBE cells. As shown in Figure 1A, there were significant increases of viral plus stranded

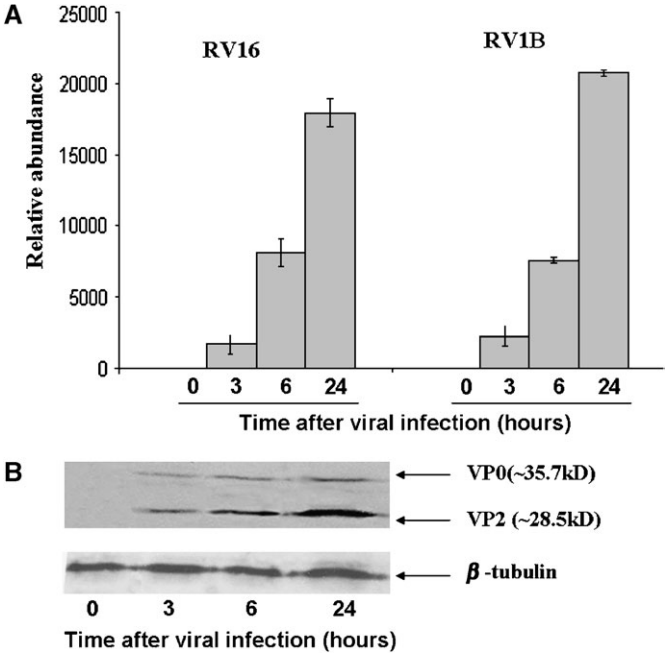

Figure 1. Characterization of viral replication in RV-infected TBE cells. Well differentiated primary human TBE cells cultured under air–liquid interface for 21 d were infected with RV16 or RV1B, as described in the text. At various times after the infection, both the apical cell surface and the basal side of the culture were washed three times with PBS, and the infected cultures were then subjected to RNA and protein extractions. (*A*) Quantitation of viral plus stranded RNA in infected cells by real-time RT-PCR with the primers specific to RV16 and RV1B, respectively. The relative abundance was calculated by the $\Delta\Delta C_t$ method, as described in MATERIALS AND METHODS. Each data point represents mean ± SD from three experiments. (*B*) Characterization of viral protein synthesis and maturation in infected cultures by Western blot analysis using a specific monoclonal antibody against RV16 coat protein (VP2). VP0 is a pro-protein that contains VP2. At the maturation step, viral protease will splice VP0 to generate VP2. Anti–β-tubulin staining was used as a loading control.

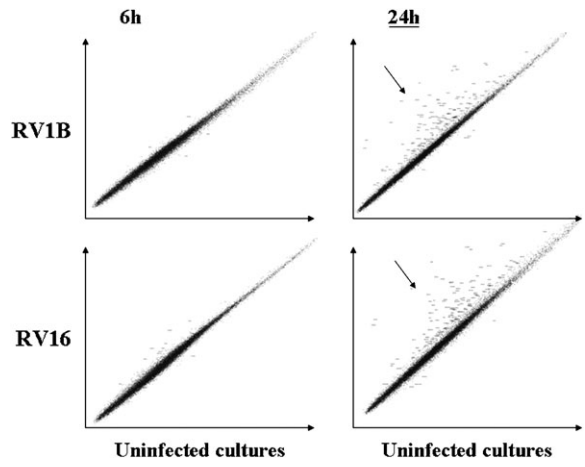

Figure 2. Representative scatter plot analyses of RV-induced gene expression by infected TBE cells. The *y*-axes represent the gene expression profiles of RV-infected cultures, whereas the *x*-axes represent the corresponding control infections with mock-infected supernatant media from cultures used for these RV stock preparations. *Arrows* indicate the genes that were significantly elevated by RV infection.

RNA at 3 h after infection. A > 20,000-fold increase of the viral RNA was observed at 24 h after infection. The time-dependent viral production was also demonstrated by the time-dependent viral coat protein synthesis in infected cells. Because no good anti-RV1B antibody is currently available, we focused on RV16 viral coat protein (VP) production in infected cultures. Western blot analysis with anti-RV16 monoclonal antibody (11) indicated that the expression of VP0 (35.7 kD) and VP2 (28.5 kD) protein was time-dependently increased up to 24 h after infection (Figure 1B). Because VP2 is generated only at the viral particle maturation step by the cleavage of VP0 (1), the increase in VP2 production reflects an increase in the production of mature viral particles. Thus, both viral RNA and viral protein data demonstrated the time-dependent RV production in primary TBE cells.

Notably, even at an MOI of 10, immunofluorescent staining using anti-RV16 antibody showed that fewer than 5% of the cultured cells were infected (data not shown). The reasons for this low infectivity in primary cells remain to be identified, but may have to do with the greater level of differentiation of cells cultured under more nearly physiologic conditions (23), and our findings are in any case quite comparable to other studies of primary epithelial cells (11).

Transcriptional Profiling of Gene Expression in RV-Infected TBE Cells by Affymetrix Genechip

Because the primary target of the RV infection is airway epithelium, we hypothesized that RV-induced airway inflammation and asthma exacerbation are initiated by the perturbation of the gene expression profile in infected airway epithelial cells. Hence, we used the state-of-the-art genechip technology to profile the global gene expression changes induced by RV infection. Because viral replication is time-dependent (Figure 1), we analyzed

TABLE 2. RHINOVIRUS-INDUCIBLE GENES

Gene	Description	Fold Induction by RV16	Fold Induction by RV1B	IFN-Related?
IFIT1	IFN-induced protein with tetratricopeptide repeat 1	21.47	17.42	y
CXCL11	Small inducible cytokine subfamily B (Cys-X-Cys), member 11	17.64	11.47	y
C1orf29	Chromosome 1 open reading frame 29	16.17	16.2	y
ISG15	IFN-stimulated protein, 15 kD	13.86	10.96	y
IFI27	IFN, α-inducible protein 27	12.44	9.78	y
Viperin	*Homo sapiens* viperin mRNA, complete cds	11.51	10.14	y
CXCL10	Small inducible cytokine subfamily B (Cys-X-Cys), member 10	11.5	6.45	y
MX1	Myxovirus (influenza virus) resistance 1, IFN-inducible protein p78 (mouse)	9.94	8.84	y
MX2	Myxovirus (influenza virus) resistance 2 (mouse)	9.01	8.21	y
G1P3	IFN, α-inducible protein (clone IFI-6–16)	8.13	10.36	y
OAS3	2′-5′-Oligoadenylate synthetase 3 (100 kD)	6.19	5.19	y
OAS2	2′-5′-Oligoadenylate synthetase 2 (69–71 kD)	6.05	5.29	y
IRF7	IFN regulatory factor 7	5.5	4.83	y
OAS1	2′,5′-Oligoadenylate synthetase 1 (40–46 kD)	4.88	4.7	y
IFITM1	IFN-induced transmembrane protein 1 (9–27 kD)	4.63	4.06	y
IFIT4	IFN-induced protein with tetratricopeptide repeats 4	4.36	4.92	y
GBP1	Guanylate binding protein 1, IFN-inducible, 67kD	4.16	3.1	y
WARS	Tryptophanyl-tRNA synthetase	4.13	2.89	y
IFIT2	IFN-induced protein with tetratricopeptide repeats 2	4.11	3.32	y
IFI35	IFN-induced protein 35	4.09	3.43	y
STAT1	Signal transducer and activator of transcription 1, 91 kD	4.08	4.07	y
IFI44	IFN-induced, hepatitis C-associated microtubular aggregate protein (44 kD)	3.84	3.77	y
MDA5	Melanoma differentiation–associated protein-5	3.5	3.47	y
ISG20	IFN-stimulated gene (20 kD)	2.82	2.4	y
OASL	2′-5′-Oligoadenylate synthetase-like	2.61	2.45	y
PKR	Protein kinase, IFN-inducible double-stranded RNA–dependent	2.3	2.34	y
ISGF3G	IFN-stimulated transcription factor 3, gamma (48 kD)	2.12	2.02	y
IFITM2	IFN-induced transmembrane protein 2 (1–8 D)	2.1	2.43	y
IFITM3	IFN-induced transmembrane protein 3 (1–8 U)	2.05	2.15	y
IFRG28	28 kD IFN-responsive protein	2.02	2.1	y
USP18	Ubiquitin specific protease 18	2.44	2.36	y
SP110	SP110 nuclear body protein	2.29	2.15	y
LAMP3	Lysosomal-associated membrane protein 3	6.06	5.53	NF*
BST2	Bone marrow stromal cell antigen 2	5.16	4.46	NF
RIG-I	RNA helicase	3.79	3.16	NF
FLJ20637	Hypothetical protein FLJ20637	3.43	3.08	NF
LOC51191	Cyclin-E binding protein 1	3.05	3.81	NF
HSXIAPAF1	XIAP associated factor-1	2.79	3.06	NF
LAP3	leucine aminopeptidase	2.69	2.61	NF
FLJ20073	Hypothetical protein FLJ20073	2.65	2.39	NF
FLJ22693	Hypothetical protein FLJ22693	2.57	2.24	NF
CIC	Capicua homolog (*Drosophila*)	2.53	2.37	NF
FLJ20035	Hypothetical protein FLJ20035	2.45	2.51	NF
APOBEC3A	Apolipoprotein B mRNA editing enzyme, catalytic polypeptide-like 3A	2.37	2.16	NF
HRASLS2	HRAS-like suppressor 2	2.3	2.14	NF
TOR1B	Torsin family 1, member B (torsin B)	2.27	2.02	NF
ECGF1	Endothelial cell growth factor 1 (platelet-derived)	2.2	1.76	NF
TRIM14	Tripartite motif-containing 14	2.19	2.06	NF

Definition of abbreviations: NF, not found to be IFN-inducible in the literature, to our knowledge; Y, IFN-inducible based on the existing literature.
* Not found by us in the literature to be IFN-inducible.

gene expression profiles at two different times: 6 and 24 h after RV infection (Figure 2). We have repeated the study on two independent cultures derived from two normal individuals. The differentially regulated genes were compared, and only the genes that had significant changes in both studies were subject to further examination. To our surprise, using a threshold of 2, we found no gene that was significantly upregulated by RV infection at 6 h after infection (Figure 2). In contrast, we found many genes were upregulated at 24 h after infection (Figure 2), but found no gene to be significantly downregulated. Interestingly, among 52 RV16-inducible genes and 51 RV1B-inducible genes, 48 were commonly induced by both RVs (Figure 2). Those three RV16-specific genes and two RV1B-specific genes were at the boundary of threshold induction (fold induction = 2.00–2.11), and their functions are unclear. Thus, it appears that both the major and the minor groups of RV induce the similar group of epithelial gene expression, at least in our system. To simplify our later studies, we used RV16 as a model to examine the signaling mechanism underlying RV-induced gene expression.

Major Innate Antiviral Systems Were Significantly Elevated in RV-Infected TBE Cells

Table 2 lists the 48 genes that were significantly induced by both RV16 and RV1B, which includes most well established antiviral systems: (*1*) PKR pathway; (*2*) coupled 2′-5′ oligoadenylate synthetase (OAS)/RNase L pathway; (*3*) Mx pathway; and (*4*) viperin.

PKR is a serine/threonine kinase and a well established central regulator in antiviral defense. PKR activation leads to its autophosphorylation and to the phosphorylation of its natural substrates, including the α subunit of eukaryotic protein synthesis initiation factor-2α, which then leads to the inhibition of protein synthesis (27). PKR can directly inhibit virus replication by inducing a set of antiviral genes, or indirectly inhibit virus replication by stimulating apoptosis of infected cells (27). In our system, PKR was significantly elevated by RV infection (Table 2).

Active OAS catalyzes the synthesis of 2′-5′–linked oligoadenylates (2′-5′A). Subsequently, the dormant cytosolic RNase L monomers are activated by forming dimers after binding 2′-5′A (28). The active RNase L endoRNase catalyzes the degradation of both viral and cellular single-stranded RNAs, thus inhibiting the translation and virus replication, and possibly also initiating apoptosis (28). In the array, all four types of OAS (OAS1, OAS2, OAS3, and OASL) were significantly elevated (Table 2), whereas the expression of RNase L remained intact. This finding appears to be consistent with the notion that the amount of OAS, but not that of RNase L, is the rate-limiting factor of this system.

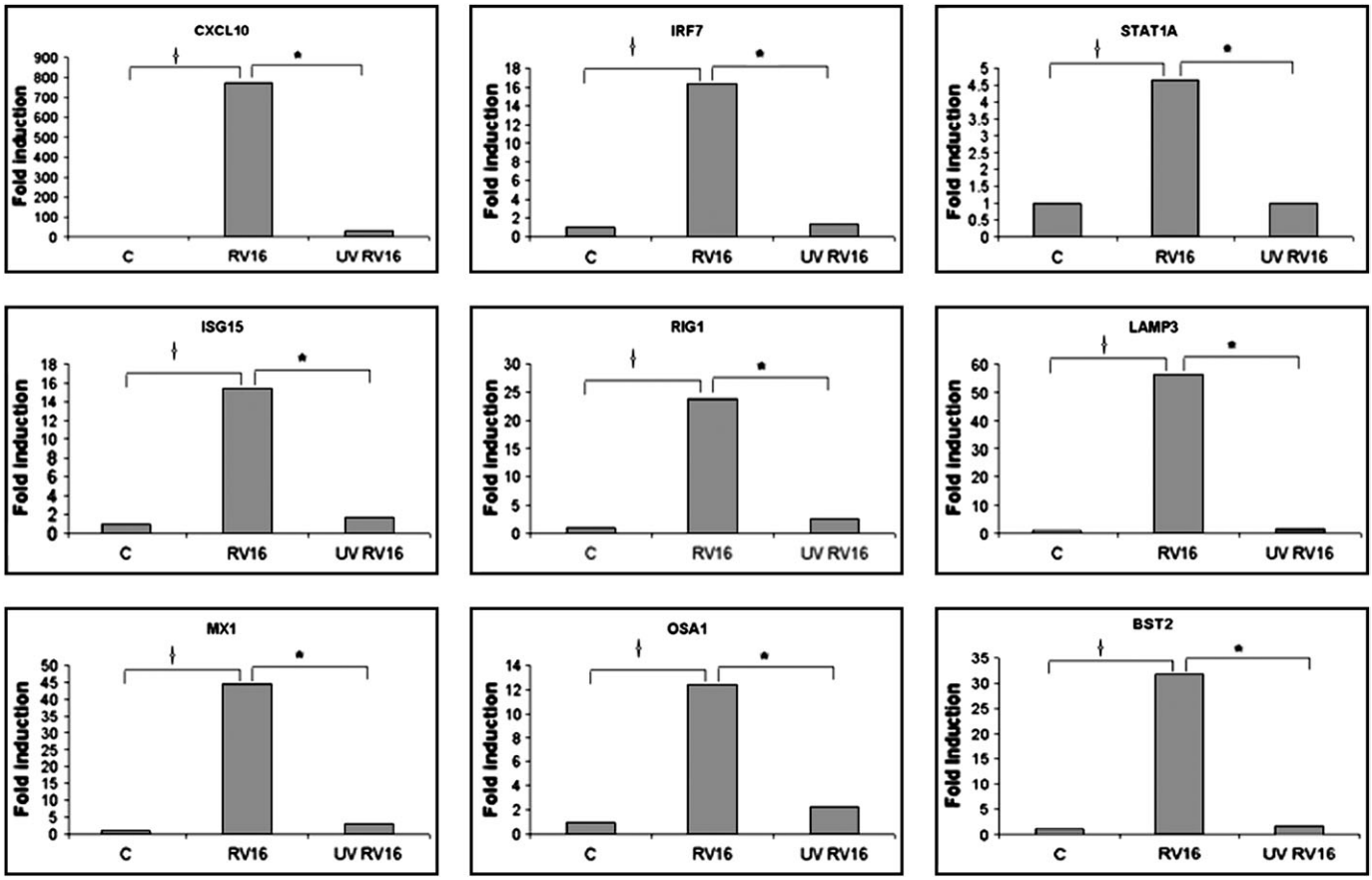

Figure 3. Real-time RT-PCR quantification of RV-induced gene expression on RV-infected and ultraviolet-irradiated RV-infected TBE cells. Primary TBE cells were infected with RV16 or ultraviolet-irradiated (UVRV16) at MOI 10, as described in the text. At 24 h after infection, cellular RNA was extracted and subjected to real-time RT-PCR analysis for these nine selected genes. Relative gene expression level for each of the selected genes was normalized with the reference gene, β-actin. Fold induction was then calculated by dividing the relative gene expression level in mock-infected control cultures. Each data point represents a mean of six repeats on the primary TBE cultures derived from a minimum of two different donors. *,† $P < 0.01$. $n = 6$.

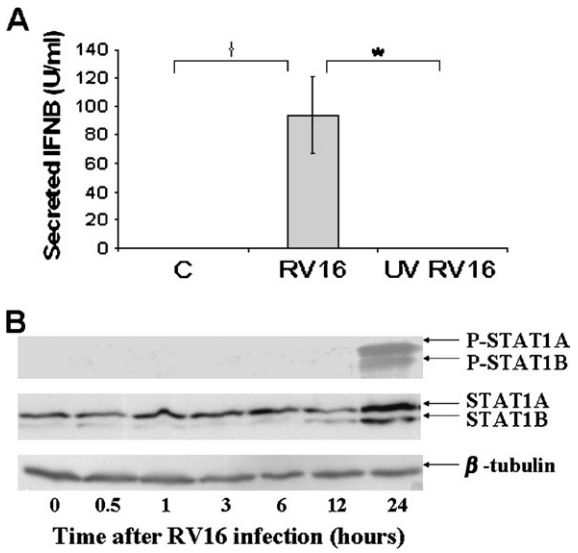

Figure 4. IFN-β production and STAT1 activation in RV-infected TBE cultures. (*A*) ELISA assay of the secreted IFN-β. Cell media were collected at 24 h after RV infection, along with the control. Concentrations of IFN-β (U/ml) were calculated based on manufacturer's instructions. Each data point represents the mean ± SD from six repeats on the primary TBE cultures derived from a minimum of two different donors. *,† $P < 0.01$; $n = 6$. (*B*) Effect of RV16 infection on STAT1 activation. Total protein was harvested at various times, as indicated, after RV16 infection. An equal amount of protein (60 μg/well) was loaded to each gel well, and equal loading was further assessed with anti–β-tubulin antibody staining. Anti–phospho-STAT1 antibody was used to probe the activated STAT1 (P-STAT1A and P-STAT1B). Anti-STAT1 antibody was used to probe the STAT1 proteins (STAT1A and STAT1B). This experiment was repeated three times.

The Mx proteins belong to the family of large GTPases. Mx protein alone is sufficient to block the replication of virus. Mx proteins can either block viral nucleocapsid transport or viral RNA synthesis (29). In our system, both subtypes of Mx protein (Mx1 and Mx2) were highly elevated (Table 2).

Viperin has been reported to be induced by human cytomegalovirus infection (30). The expression of viperin inhibits viral infection by inhibiting viral proteins that are required for viral assembly and maturation (30). In our system, viperin was highly elevated (Table 2).

Majority of the RV-Induced Genes Are IFN-Related

Interestingly, all the antiviral genes mentioned above have previously been demonstrated as IFN-stimulated genes (ISG). Aside from these genes, 32 of the 48 RV-inducible genes (as indicated by "y" in Table 2) appear to link directly to the IFN pathway. Among them, *ISG20*, *ISG15*, *IFRG28*, *IFITM1*, *IFIT4*, *IFIT2*, *IFIT1*, *IFI44*, *IFI35*, *IFI27*, *GBP1*, and *G1P3* were identified previously by a differential hybridization protocol comparing IFN-treated and untreated cultures. Two IFN-inducible chemokines (CXCL10 and CXCL11) were also found to be highly elevated in RV-infected cultures. The major function of those two chemokines is to recruit catalytic T lymphocytes, and they appear to serve as messengers to call upon the adaptive immune response to combat the invading virus. Besides these downstream effectors, the signaling molecules in the IFN pathway, such as *STAT1*, *ISGF3G*, and *IRF7*, were also significantly elevated at 24 h after RV infection (Table 2).

Real-Time RT-PCR Quantification and Viral RNA Replication-Dependent Elevation of the RV-Inducible Genes

To simplify the signaling transduction studies, nine representative RV-inducible genes of different categories: *CXCL10*, *BST2*, *ISG15*, *STAT1A*, *RIG1*, *IRF7*, *LAMP3*, *Mx1*, and *OAS1*, were selected for further quantitative RT-PCR analysis in our later studies. *CXCL10* represents the inducible chemokine, whereas *ISG15* represents the classic ISGs that were identified previously by differential display (32). *OAS1* and *Mx1* represent the well characterized antiviral systems. *STAT1* and *IRF7* represent the signaling molecules in the IFN pathway. *BST2*, *RIG1*, and *LAMP3* represent the RV-inducible genes that haven't been reported in the literature as ISGs. Real-time RT-PCR approach confirmed the induction of these genes in TBE cultures after RV infection (Figure 3). These inductions varied from 5- (*STAT1A*) to 700-fold (*CXCL10/IP10*) among these 9 genes. These inductions appear to be dependent on viral RNA replication, as no induction of these genes (Figure 3) was observed in TBE cells infected with ultraviolet-irradiated RV16.

IFN-β Is the Major Bioactive IFN Induced by RV16 Infection on TBE Cells

Because a large portion of those RV-inducible genes are ISGs, we determined whether the IFN molecules were induced by RV and were responsible for the induction of the ISGs in this study. To address this question, the ELISA method was used to measure the IFN production in RV-16–infected TBE cells and mock-infected cells. No IFN-α and IFN-γ was identified by the ELISA assay at their detection limits (2 U/ml for IFN-α and 0.08 U/ml for IFN-γ), respectively. Notably, the IFN-α ELISA kit can detect multiple subtypes of IFN-α. Thus, it appears that TBE cells do not produce detectable amounts of IFN-α and IFN-γ under either infected or mock-infected conditions. In contrast, we were able to detect the increased secretion of IFN-β in TBE cells after RV16 infection (Figure 4A). At 24 h after infection, IFN-β was secreted at 93 ± 27 U/ml, whereas no IFN-β was detected in the mock-infected culture.

We then asked whether the RV-induced IFN-β could elicit any intracellular signal. To elicit intracellular signal, IFN must bind the type I IFN receptor, activate JAK, and then phosphorylate STAT1. The phosphorylated STAT1 will then translocate into the nucleus to activate gene transcription (32). Thus, we used the STAT1 phosphorylation as a marker of IFN-induced intracellular signaling. Indeed, STAT1 phosphorylation was observed in TBE cells at 24 h after RV infection (Figure 4B). Consistent with the elevation of STAT1 mRNA in the gene profiling data (Table 2), both STAT1A and STAT1B proteins were also elevated in TBE cells 24 h after infection.

Altogether, RV-induced IFN-β is the major IFN secreted by TBE cells that is capable of inducing cellular signaling in an autocrine/paracrine manner.

Effect of IFN-β Autocrine/Paracrine Pathway on RV-Induced Gene Expression

As mentioned above, to elicit intracellular signal, the secreted IFN-β must bind the type I IFN receptor and activate JAK. Therefore, to further elaborate the role of IFN-β autocrine/paracrine signaling in RV-induced gene expression, a neutralizing antibody against IFN-β (IFNBab) (Figure 5) and a specific inhibitor blocking JAK activity (Figure 6) were used in the study. Similar to Figure 3, the real-time RT-PCR approach confirmed the induction of these nine selected genes in TBE cultures after RV infection. The treatment of IFNBab had significant inhibitory effects on all RV-induced gene expressions (Figure 5); and the degree of inhibition was different, ranging from 22–75%.

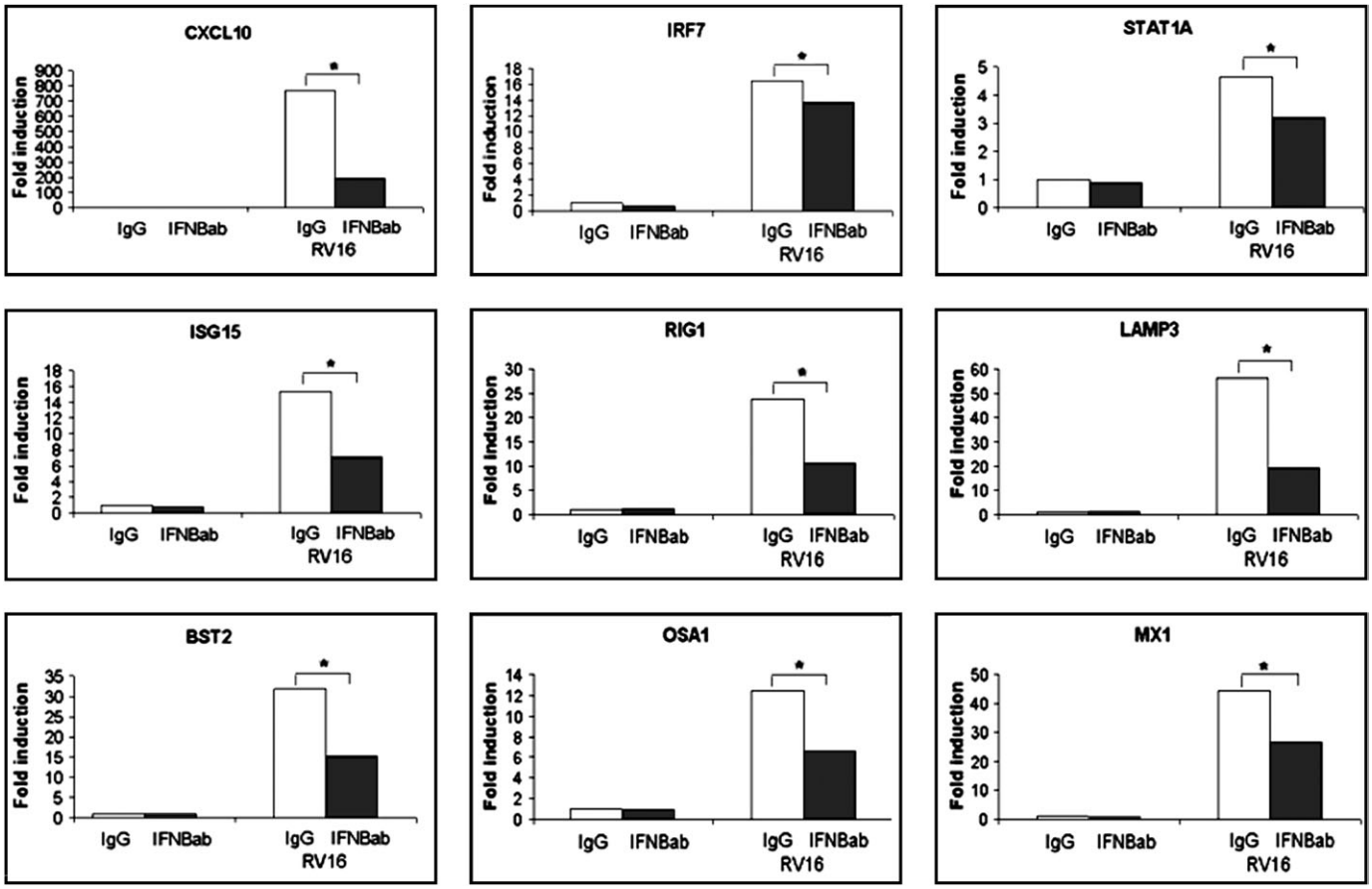

Figure 5. Effects of neutralizing antibody against IFN-β (INFBab) on RV-induced gene expression. At 1 h before RV16 infection, primary TBE cells were treated with IFNBab (20 μg/ml). Type-matched unrelated antibody (IgG) was used as a control. Total RNAs were isolated 24 h after RV infection and subjected to real-time RT-PCR analysis of these nine selected RV-induced genes. Fold induction was calculated as described in the legend for Figure 3. Each data point represents a mean from six repeats on the primary TBE cultures derived from a minimum of two different donors. *$P < 0.01$; $n = 6$.

Notably, the initial concentrations of IFNBab (20ug/ml) were selected based on the blocking curve from the data sheet of R&D Systems Inc. At this dose, we observed that IFNBab inhibited CXCL10 expression by 95%, and ISG15 expression by 90%, in TBE cells treated with IFN-β (100 U/ml) (data not shown).

Consistent with these antibody studies, a specific pan-JAK inhibitor (JAK inhibitor I) that can block the activation of all four JAK kinase family members (JAK1, JAK2, JAK3, and TYK2) also partially blocked the RV-induced gene expression at the 0.1 or 0.3 μM level. At the highest dose (1 μM), the blocking effect was more complete (Figure 6). To access the potential toxic effect of JAK inhibitor I, we measured LDH release under both RV-infected and uninfected cells that were also treated with the inhibitor. For uninfected cells, JAK inhibitor I caused certain cytotoxicity, as indicated by an increased LDH release (Table 3), which was consistent with the slight decrease of basal gene expression level (Figure 6). However, RV infection caused much more severe cell death, and no additive toxicity was observed in cells that were also treated with the inhibitor (Table 3). Thus, the inhibition of RV-induced gene expression by JAK inhibitor I could not be attributed to its toxic effect.

Collectively, these results suggest that the autocrine/paracrine IFN-β signaling pathway plays a role in RV-induced gene expression. However, the partial effect of the IFN-β neutralizing antibody, even at the high dose, suggests that other pathways may be present.

Effects of dsRNA-Mediated Pathway in RV-Induced Gene Expression

To explore the additional signaling mechanism, we considered the viral component as a potential candidate. RV is a very simple plus-stranded virus with only viral genomic RNA in the virion. Previous report has suggested that dsRNA, generated from viral replication, can induce robust cellular responses (34). Here, we found that RV replication generated an enormous amount of RNA in the infected cells (Figure 1A). Therefore, we tested the hypothesis that dsRNA-dependent signaling is responsible for RV-induced gene expression. First, since dsRNA was generated by viral replication, replication deficient virus (such as ultraviolet-irradiated RV) would not generate any dsRNA. Indeed, as shown before in Figure 3, the infection with the ultraviolet-irradiated RV did not upregulate expression of any RV-inducible genes. Second, all selected RV-inducible genes were significantly induced by the direct treatment of the synthetic dsRNA analog (poly IC) (Table 4). Third, because dsRNA has been widely reported to induce gene expression through the activation of PKR activity, we decided to examine the role of PKR in this RV-induced gene expression. By using a specific PKR inhibitor (2-AP), RV-induced gene expression was almost completely

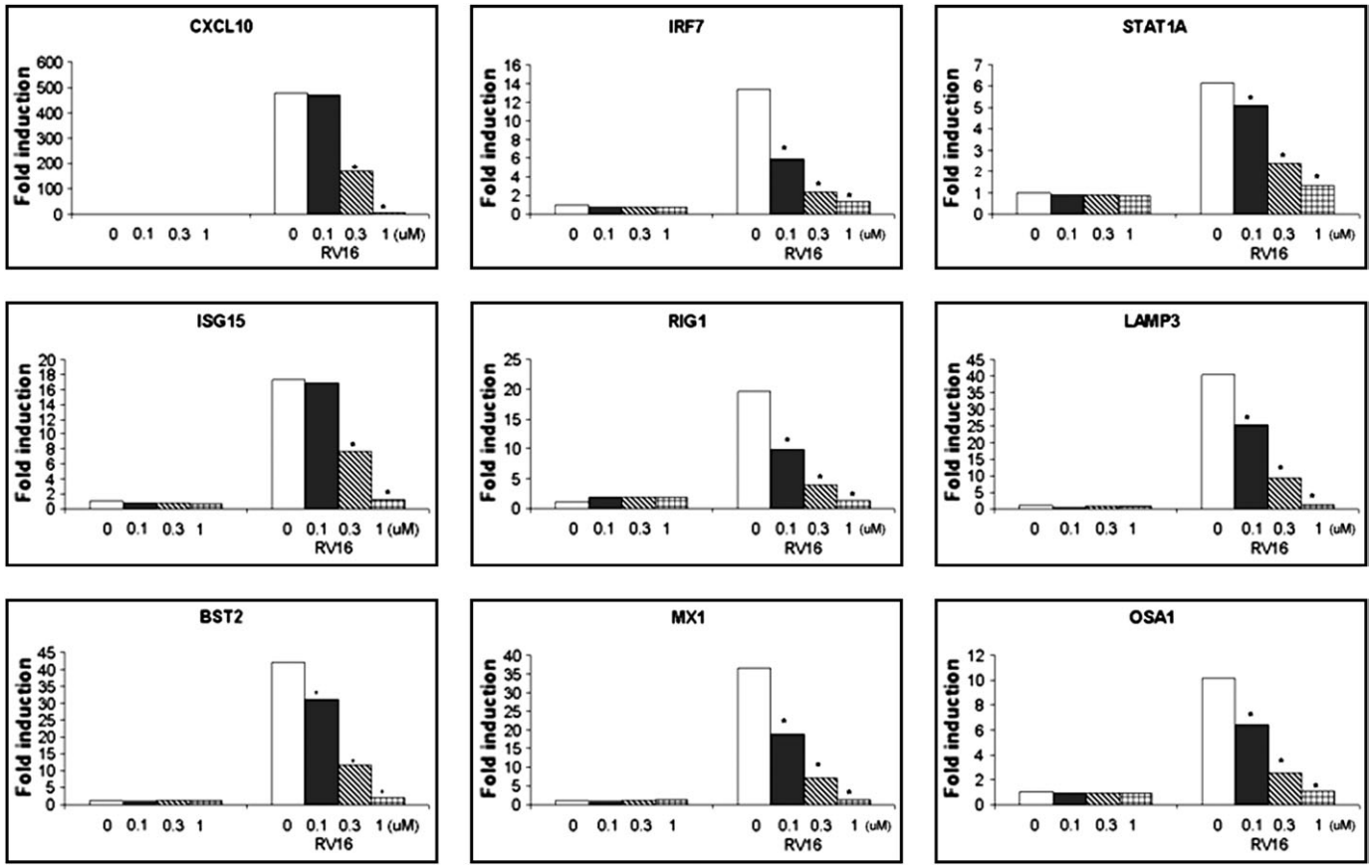

Figure 6. Effect of pan-JAK inhibitor (JAK inhibitor I) on RV16-induced gene expression. At 1 h before RV16 infection, primary TBE cells were treated with JAK inhibitor I at 0.1, 0.3, and 1 μM. Total RNAs were isolated 24 h after RV infection and subjected to real-time RT-PCR analysis of these nine selected RV-induced genes. Fold induction was calculated as described in the legend for Figure 3. Each data point represents a mean of six repeats on the primary TBE cultures derived from a minimum of two different donors. Comparison was made between RV-infected cells without inhibitor treatment and RV-infected cells with inhibitor treatment at various doses. *$P < 0.01$; $n = 6$.

blocked (Figure 7). To access the potential toxic effect of 2-AP, we measured LDH release under both RV-infected and uninfected cells that were also treated with the inhibitor. For uninfected cells, 2-AP caused a certain degree of cytotoxicity, as indicated by an increased LDH release (Table 3), which was consistent with the slight decrease of basal gene expression level (Figure 7). However, RV infection caused much more severe cell death, and no additive toxicity was observed in cells that were also treated with the inhibitor (Table 3). Thus, the inhibition of RV-induced gene expression by 2-AP could not be attributed to its toxic effect.

Because the literature suggests that the dsRNA-dependent PKR pathway can induce IFN secretion, we tested the potential cross-talk between the PKR pathway and the IFN-β autocrine/paracrine pathway. As shown in Figure 8A, 2-AP blocked the secretion of IFN-β. Consistently, 2-AP almost completely abolished the activation of PKR and STAT1 (Figure 8B). In contrast, IFNBab had no effect on the PKR activation, and only partially repressed STAT1 activation (Figure 8B), which could explain the incomplete inhibition by IFNBab of those RV-inducible genes (Figure 5).

These results demonstrate that the dsRNA-dependent PKR pathway is upstream of the IFN-β autocrine/paracrine pathway in RV-induced gene expression.

Disruption of Antiviral Pathway–Enhanced RV Production

As shown in Figures 6 and 7, a PKR inhibitor (2-AP) and a pan-JAK inhibitor (JAK inhibitor I) could significantly block cellular antiviral response. Thus, we tested whether the disruption of antiviral pathway could cause the increase of RV production.

TABLE 3. LACTATE DEHYDROGENASE (LDH) ASSAY

Treatment	C	2-AP	JAK	RV	RV + 2-AP	RV + JAK
Percentage of cell death	7.63 ± 4.28	15.58 ± 4.04	11.20 ± 2.36	43.00 ± 6.09	43.04 ± 8.23	35.78 ± 8.66

Definition of abbreviations: 2-AP, 2-aminopurine; C, control; JAK, Janus kinase; RV, rhinovirus.

Detailed protocol is described in Materials and Methods. Samples were collected after 24-h treatment. All data are percentage of cell death, presented as mean ± SD, n = 4. 2-AP, cells treated with 2-AP only; JAK, cells treated with JAK inhibitor I only; RV, cells infected with RV only; RV+2-AP, RV-infected cells with 2-AP treatment; RV+JAK, RV-infected cells with JAK inhibitor I treatment.

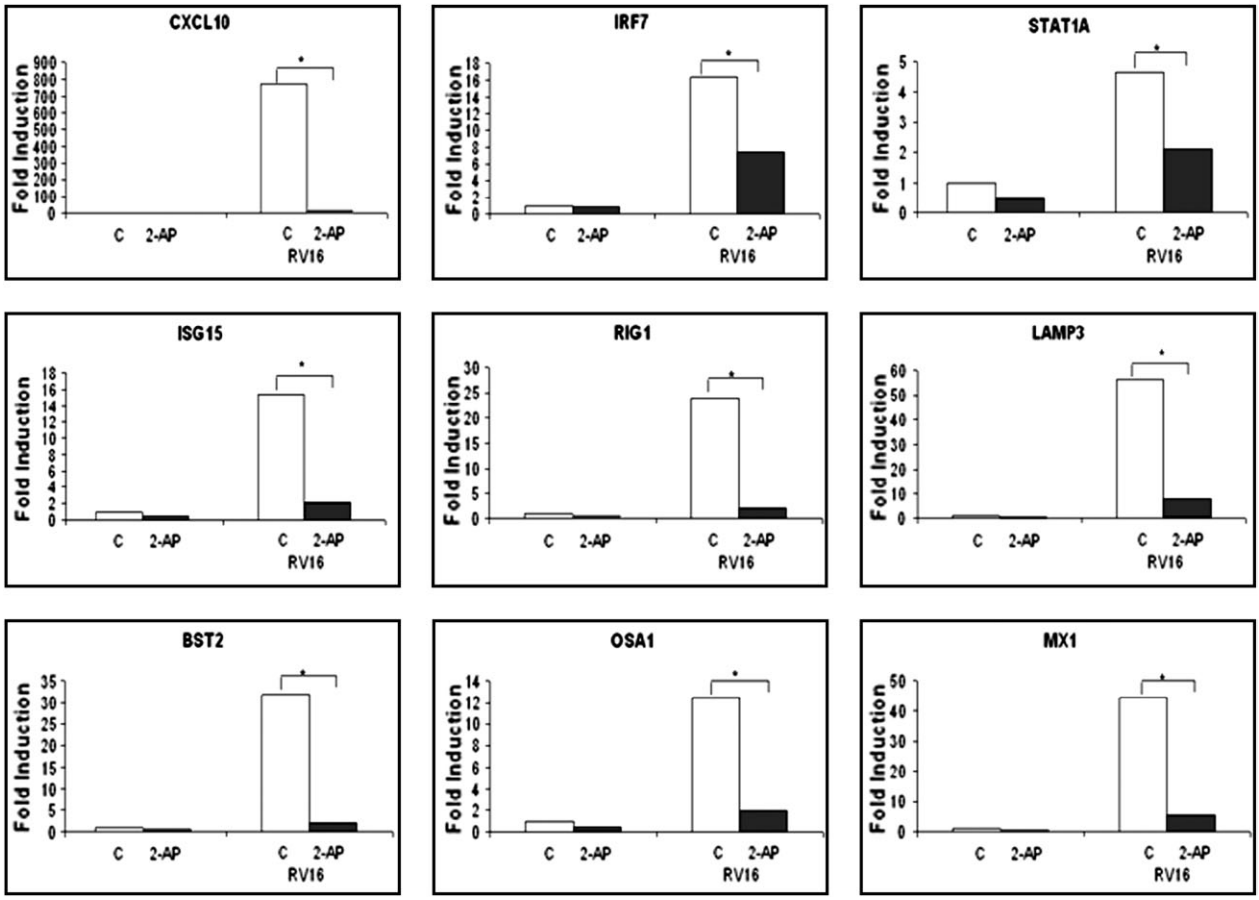

Figure 7. Effects of 2-AP on RV16-induced gene expression. At 1 h before RV16 infection, primary TBE cells were treated with 2-AP at 2 mM. Total RNAs were isolated 24 h after RV infection and subjected to real-time RT-PCR analysis of these nine selected RV-induced genes. Fold induction was calculated as described in the legend for Figure 3. Each data point represents a mean of six repeats on the primary TBE cultures derived from a minimum of two different donors. *$P < 0.01$; $n = 6$.

Indeed, both inhibitors significantly increased intracellular viral VP2 protein (Figures 9A and 9B) and viral production (Figure 9C). This finding further confirms the importance of PKR and JAK signaling pathway in cellular antiviral responses.

DISCUSSION

In this study, we performed gene expression profiling analysis in RV-infected, well differentiated primary human TBE cells *in vitro*. We have identified 48 cellular genes that were significantly elevated by both RV16 and RV1B. The results were further confirmed by real-time RT-PCR. The genes induced by infection with either the major group (RV16) or the minor group (RV1B) of RV were quite similar.

TABLE 4. GENE EXPRESSION INDUCED BY SYNTHETIC DOUBLE-STRANDED RNA (POLY-IC, 25 μg/ml). FOLD INDUCTION OF SELECTIVE RV-INDUCIBLE GENES BY DOUBLE-STRANDED RNA (25 μg/ml) TREATMENT

Genes	Fold Induction
CXCL10	1,468 ± 121
BST2	23 ± 4
ISG15	110 ± 21
STAT1A	7 ± 2
RIG1	16 ± 3
IRF7	31 ± 5
LAMP3	50 ± 4
MX1	39 ± 11
OAS1	24 ± 6

We found that primary TBE cells appeared to be resistant to RV infection. We observed very low infectivity of RV16 (< 5%) on well differentiated primary TBE cells at an MOI of 10; in contrast, cell lines such, as HBE1 or BEAS-2B, have much higher susceptibility (~ 100%) at a similar MOI. Consistent with this finding, a recent article reported by our colleague Lopez-Souza and coworkers (23) demonstrated that well differentiated cells have low susceptibility to RV infection in comparison with the poorly differentiated cells.

Despite the low RV infectivity in our system, we have identified 48 cellular genes that were highly elevated by RV infection. Although many of those genes have been reported previously in other viral infections, such as respiratory syncytial virus (RSV), HIV, etc., they have never been identified before as RV-inducible genes in human airway epithelial cells. Most RV-inducible genes have direct or indirect antiviral activity, as described in RESULTS. The general theme of these RV-inducible genes is to control the viral infection by: (*1*) inhibition of viral production by attacking multiple steps in the viral life cycles (MX1, OAS1, viperin); (*2*) enhancement of apoptosis of the infected cells (PKR); (*3*) secretion of chemokines (CXCL10 and

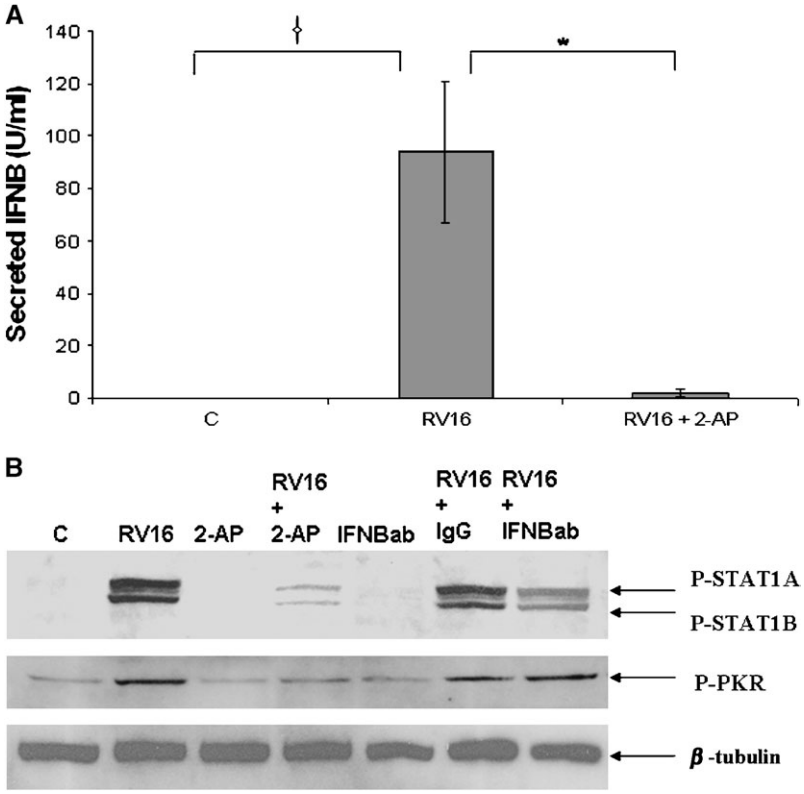

Figure 8. Induction of IFN-β autocrine/paracrine pathway by PKR activation. (*A*) Effect of 2-AP on IFN-β secretion. 2-AP treatment was performed as described in the legend for Figure 7. Cell media were collected at 24 h after RV infection, along with the control. Concentrations of IFN-β (U/ml) were calculated based on manufacturer's instructions. Each data point represents the mean ± SD from six repeats on the primary TBE cultures derived from a minimum of two different donors. Because the detection limit was 1 U/ml, 1 U/ml was arbitrarily assigned to any undetectable samples for the comparison. $^{*,\dagger}P < 0.01$. $n = 6$. (*B*) Western analysis of the effects of 2-AP and IFN-Bab on the activation of STAT1 and PKR. Total protein was harvested at various times, as indicated, after RV16 infection. An equal amount of protein (60 μg/well) was loaded on each gel well, and equal loading was further assessed with anti–β-tubulin antibody staining. Anti–phospho-STAT1 antibody was used to probe the activated STAT1 (P-STAT1A and P-STAT1B). Anti–phosphor-PKR antibody was used to probe the activated PKR protein. This experiment was repeated three times.

CXCL11) that facilitate the recruitment of cytolytic T cells to remove the infected cells.

Because many RV-induced genes are related in terms of IFN inducibility and antiviral function, we have asked whether a common pathway is responsible for RV-induced gene expression. Indeed, based on the studies using neutralizing antibody and specific chemical inhibitors, we found that both a dsRNA-PKR–dependent pathway and its induced IFN-β autocrine/paracrine–mediated JAK-STAT pathway are involved in the RV-induced gene expression (Figure 10).

Based on the blocking studies, the dsRNA-PKR pathway appears to be the major signaling pathway induced by RV infection. We have also found that dsRNA *per se* could robustly elevate similar gene expression in the absence of real viral infection. It is unclear as to how much dsRNA must be generated in the RV-infected cells to exert gene induction; likewise, it is also unclear how much synthetic dsRNA (e.g., polyIC) actually gets into the cells to initiate signaling. Another study (33) indicated that a much lower dose of dsRNA would be needed if it was transfected into, rather than directly applied onto, the cells. This supports the notion that very few copies of dsRNA are actually required to initiate PKR signaling. It is interesting to note that all the asthma-exacerbating viruses (such as RV, respiratory syncytial virus (34), and influenza) generate dsRNA in their life cycles.

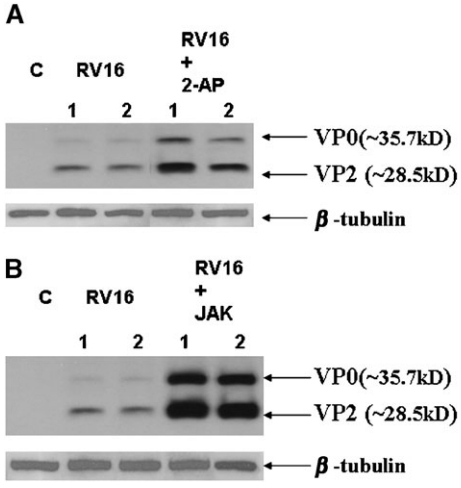

C Viral yield (Log_{10}TCID50 /ml)

	Titer
RV	5.56 ± 0.28
RV+2-AP	6.10 ± 0.25*
RV+JAK	6.85 ± 0.58*

Figure 9. Disruption of antiviral pathway enhanced RV production. Inhibitor treatments were performed as described in the legends for Figures 6 and 7. Cells were infected by RV for 24 h. Cell surfaces were then completely washed and replaced with fresh medium. After 24 h, viral production was determined by both Western blot analysis on cellular protein and $TCID_{50}$ assay on culture media. (*A*) Western analysis of 2-AP effect on RV production. Two independent samples (labeled as *1* and *2*) were loaded on the same gel. A total of four independent samples were examined. A specific monoclonal antibody against RV16 coat protein (VP2) was used for Western blot analysis. VP0 is a pro-protein that contains VP2. Anti–β-tubulin staining was used as a loading control. (*B*) Western analysis of the effect of JAK inhibitor I (JAK) on RV production. (*C*) $TCID_{50}$ assay was used to measure extracellular viral yield. Apical viral titer listed in the table is mean ± SD. Basal viral titer was undetectable. $^{*}P < 0.05$; $n = 4$.

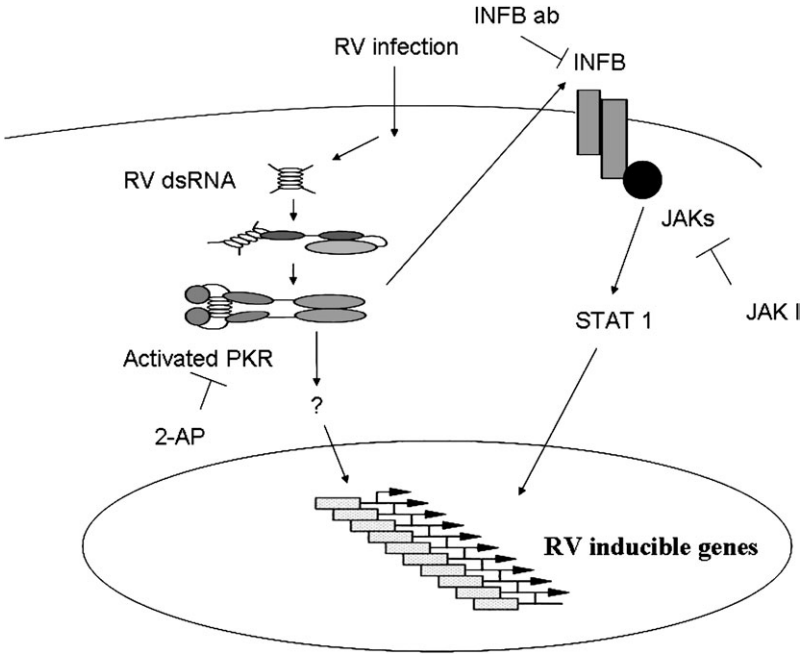

Figure 10. Diagram summarizing the signaling transduction pathways involved in RV-induced gene expression in primary human TBE cells infected with RV16. The replication of viral RNA leads to the formation of dsRNA. dsRNA activates PKR, which is responsible for the induction of RV-inducible genes through an unidentified mechanism (indicated as "?"). The activation of PKR also induces the secretion of IFN-β. The secreted IFN-β binds to the type I IFN receptor in an autocrine/paracrine fashion, which leads to the activation of the JAK-STAT pathway and the stimulation of RV-inducible genes. Various inhibitors and antibody used in this study, and their corresponding inhibitory steps, are indicated in this diagram.

Therefore, it would be fruitful to continue the study of the role of dsRNA in airway inflammatory responses and asthma exacerbations.

We have also shown that RV infection can induce IFN-β secretion, which appears to have a partial effect on the RV-induced gene expression. This finding is consistent with the long-held belief that the dsRNA-PKR pathway can activate IFN production in many other cell types (27). Interestingly, one most recent study (18) has demonstrated the causal linkage between an impairment of RV-induced IFN-β production in asthmatic airway epithelial cells and an increase in RV production from those cell cultures. Their finding is consistent with our result regarding the IFN-β effect on antiviral gene expression. However, we did not observe the induction of IFN-β mRNA in the Genechip assays, despite the presence of the corresponding probe sets on the chips. Thus, RV might induce IFN-β secretion without significant elevation of its transcription. Or, the IFN-β probe sets on the chips were just not appropriate for this detection; and the latter emphasizes the importance of using other molecular and biochemical methods to corroborate and complement the Genechip study, as we did in this study. Although the autocrined/paracrined IFN-β had only a partial effect on RV-induced epithelial gene expression, it might also act on other cell types *in vivo*. In addition, our results have shown that several key IFN signal molecules (STAT1A, ISGF3G, and IRF7) were highly elevated, which may indicate the high alert status of the IFN system in RV-infected cells. Because many cell types (e.g., macrophages, T lymphocytes, etc.) in the airway are capable of secreting a large amount of IFN, the RV-infected epithelia may manifest a much more robust IFN response with the exogenous IFN challenge *in vivo*. Is it possible that the overzealous epithelial IFN response (or antiviral response) is involved in asthma exacerbation? Two recent studies from Holtzman and colleagues supported this notion. Using human asthmatic tissue samples, they have demonstrated that STAT1, a key IFN signaling molecule, is highly elevated and activated in the asthmatic airways (35). The second study, using a Sendai-virus infection mouse model, further demonstrated that viral infection itself can cause many aspects of asthmatic symptoms (36).

Because RV-induced genes were mostly related to antiviral response, and the PKR–IFN-β–JAK–STAT pathway was responsible for their induction, we further tested whether the disruption of this pathway could affect viral production. As expected, both PKR inhibitor (2-AP) and pan-JAK inhibitor (JAK inhibitor I), which had inhibitory effects on antiviral gene expression, significantly enhanced viral production. Interestingly, a recent study has demonstrated that, because of a deficiency of epithelial antiviral response, asthmatic airway epithelial cells could produce much more virus than normal cells upon RV infection (18). Thus, alteration of epithelial antiviral defense in the diseased condition might contribute to the pathogenesis of airway disease exacerbations.

To our surprise, we did not find any robust elevations of the previously reported cytokine genes, such as IL-6 and IL-8 (12–15). This is not due to the lack of sensitivity of the Genechip technique, because subsequent ELISA analysis showed at most a marginal and inconsistent elevation of IL-6 and IL-8 after RV infection (data not sown). We examined the idea that expression of IL-6 and IL-8 is a function of the proportion of cells infected by varying the dose RV in the inoculum. When we increased the infecting dose to an MOI of 100, more than 70% of the cells were infected, and IL-6 and IL-8 expression was significantly induced. However, to achieve an MOI of 100, we needed to use the virus stock at 10^8 PFU/well, a level that may never occur physiologically, and that presents a daunting challenge to the researcher. Thus, even though the cytokines are significantly elevated in airway secretions from patients with community-acquired or experimentally-induced RV infections, whether they are actually produced by epithelial cells under these conditions remains to be determined.

In summary, we have reported the first gene expression profile analysis in well differentiated human airway epithelial cells after RV infection in a well controlled *in vitro* environment. We have demonstrated two interacting signaling pathways involved in RV-induced gene expression. Deactivation of these pathways can significantly increase epithelial viral production. This new information will significantly advance our understanding of the

pathogenesis of RV infection. Full understanding of the RV-induced airway epithelial response is the first key step to uncovering the pathogenesis of the RV-induced common cold and asthma exacerbations. Because of the broad disease prevalence and the high financial burden, these studies have the potential for great impact on the human health.

Conflict of Interest Statement: None of the authors has a financial relationship with a commercial entity that has an interest in the subject of this manuscript.

Acknowledgments: The authors express their thanks to Yuhua Zhao for technical assistance with cell cultures, Dr. James E. Gern (University of Wisconsin, Madison) for providing the monoclonal antibody against RV16, and Dr. Jonathan Widdicombe for the discussion about electro-properties of TBE cells.

References

1. Savolainen C, Blomqvist S, Hovi T. Human rhinoviruses. *Paediatr Respir Rev* 2003;4:91–98.
2. Makela MJ, Puhakka T, Ruuskanen O, Leinonen M, Saikku P, Kimpimaki M, Blomqvist S, Hyypia T, Arstila P. Viruses and bacteria in the etiology of the common cold. *J Clin Microbiol* 1998;36:539–542.
3. Temte JL. A family physician's perspective on picornavirus infections in primary care. *Arch Fam Med* 2000;9:921–922.
4. Busse WW, Gern JE. Viruses in asthma. *J Allergy Clin Immunol* 1997; 100:147–150.
5. Johnston SL, Pattemore PK, Sanderson G, Smith S, Lampe F, Josephs L, Symington P, O'Toole S, Myint SH, Tyrrell DA, *et al.* Community study of role of viral infections in exacerbations of asthma in 9–11 year old children. *BMJ* 1995;310:1225–1229.
6. Nicholson KG, Kent J, Ireland DC. Respiratory viruses and exacerbations of asthma in adults. *BMJ* 1993;307:982–986.
7. Johnston SL, Pattemore PK, Sanderson G, Smith S, Campbell MJ, Josephs LK, Cunningham A, Robinson BS, Myint SH, Ward ME, *et al.* The relationship between upper respiratory infections and hospital admissions for asthma: a time trend analysis. *Am J Respir Crit Care Med* 1996;154:654–660.
8. Gern JE, Dick EC, Lee WM, Murray S, Meyer K, Handzel ZT, Busse WW. Rhinovirus enters but does not replicate inside monocytes and airway macrophages. *J Immunol* 1996;156:621–627.
9. Halperin SA, Eggleston PA, Hendley JO, Suratt PM, Groschel DH, Gwaltney JM Jr. Pathogenesis of lower respiratory tract symptoms in experimental rhinovirus infection. *Am Rev Respir Dis* 1983;128:806–810.
10. Gern JE, Galagan DM, Jarjour NN, Dick EC, Busse WW. Detection of rhinovirus RNA in lower airway cells during experimentally induced infection. *Am J Respir Crit Care Med* 1997;155:1159–1161.
11. Mosser AG, Brockman-Schneider R, Amineva S, Burchell L, Sedgwick JB, Busse WW, Gern JE. Similar frequency of rhinovirus-infectible cells in upper and lower airway epithelium. *J Infect Dis* 2002;185:734–743.
12. Schroth MK, Grimm E, Frindt P, Galagan DM, Konno SI, Love R, Gern JE. Rhinovirus replication causes RANTES production in primary bronchial epithelial cells. *Am J Respir Cell Mol Biol* 1999;20:1220–1228.
13. Johnston SL, Papi A, Bates PJ, Mastronarde JG, Monick MM, Hunninghake GW. Low grade rhinovirus infection induces a prolonged release of IL-8 in pulmonary epithelium. *J Immunol* 1998;160:6172–6181.
14. Papadopoulos NG, Papi A, Meyer J, Stanciu LA, Salvi S, Holgate ST, Johnston SL. Rhinovirus infection up-regulates eotaxin and eotaxin-2 expression in bronchial epithelial cells. *Clin Exp Allergy* 2001;31:1060–1066.
15. Kim J, Sanders SP, Siekierski ES, Casolaro V, Proud D. Role of NF-kappa B in cytokine production induced from human airway epithelial cells by rhinovirus infection. *J Immunol* 2000;165:3384–3392.
16. Douglas RG Jr, Cate TR, Gerone PJ, Couch RB. Quantitative rhinovirus shedding patterns in volunteers. *Am Rev Respir Dis* 1966;94:159–167.
17. Douglas RG Jr, Alford BR, Couch RB. Atraumatic nasal biopsy for studies of respiratory virus infection in volunteers. *Antimicrob Agents Chemother* 1968;8:340–343.
18. Wark PA, Johnston SL, Bucchieri F, Powell R, Puddicombe S, Laza-Stanca V, Holgate ST, Davies DE. Asthmatic bronchial epithelial cells have a deficient innate immune response to infection with rhinovirus. *J Exp Med* 2005;201:937–947.
19. Wang W, Lee WM, Mosser AG, Rueckert RR. WIN 52035–dependent human rhinovirus 16: assembly deficiency caused by mutations near the canyon surface. *J Virol* 1998;72:1210–1218.
20. Duits LA, Nibbering PH, van Strijen E, Vos JB, Mannesse-Lazeroms SP, van Sterkenburg MA, Hiemstra PS. Rhinovirus increases human beta-defensin-2 and -3 mRNA expression in cultured bronchial epithelial cells. *FEMS Immunol Med Microbiol* 2003;38:59–64.
21. Chen Y, Zhao YH, Di YP, Wu R. Characterization of human mucin 5B gene expression in airway epithelium and the genomic clone of the amino-terminal and 5′-flanking region. *Am J Respir Cell Mol Biol* 2001;25:542–553.
22. Wu R, Zhao YH, Chang MM. Growth and differentiation of conducting airway epithelial cells in culture. *Eur Respir J* 1997;10:2398–2403.
23. Lopez-Souza N, Dolganov G, Dubin R, Sachs LA, Sassina L, Sporer H, Yagi S, Schnurr D, Boushey HA, Widdicombe JH. Resistance of differentiated human airway epithelium to infection by rhinovirus. *Am J Physiol Lung Cell Mol Physiol* 2004;286:L373–L381.
24. Irizarry RA, Bolstad BM, Collin F, Cope LM, Hobbs B, Speed TP. Summaries of Affymetrix GeneChip probe level data. *Nucleic Acids Res* 2003;31:e15.
25. Kao CY, Chen Y, Thai P, Wachi S, Huang F, Kim C, Harper RW, Wu R. IL-17 markedly up-regulates beta-defensin-2 expression in human airway epithelium via JAK and NF-kappaB signaling pathways. *J Immunol* 2004;173:3482–3491.
26. Deng J, Chen Y, Wu R. Induction of cell cornification and enhanced squamous-cell marker SPRR1 gene expression by phorbol ester are regulated by different signaling pathways in human conducting airway epithelial cells. *Am J Respir Cell Mol Biol* 2000;22:597–603.
27. Williams BR. PKR: a sentinel kinase for cellular stress. *Oncogene* 1999; 18:6112–6120.
28. Castelli J, Wood KA, Youle RJ. The 2–5A system in viral infection and apoptosis. *Biomed Pharmacother* 1998;52:386–390.
29. Haller O, Kochs G. Interferon-induced mx proteins: dynamin-like GTPases with antiviral activity. *Traffic* 2002;3:710–717.
30. Chin KC, Cresswell P. Viperin (cig5), an IFN-inducible antiviral protein directly induced by human cytomegalovirus. *Proc Natl Acad Sci USA* 2001;98:15125–15130.
31. Clauss IM, Wathelet MG, Szpirer J, Content J, Islam MQ, Levan G, Szpirer C, Huez GA. Chromosomal localization of two human genes inducible by interferons, double-stranded RNA, and viruses. *Cytogenet Cell Genet* 1990;53:166–168.
32. Darnell JE Jr, Kerr IM, Stark GR. Jak-STAT pathways and transcriptional activation in response to IFNs and other extracellular signaling proteins. *Science* 1994;264:1415–1421.
33. Gern JE, French DA, Grindle KA, Brockman-Schneider RA, Konno S, Busse WW. Double-stranded RNA induces the synthesis of specific chemokines by bronchial epithelial cells. *Am J Respir Cell Mol Biol* 2003;28:731–737.
34. Zhao J, Takamura M, Yamaoka A, Odajima Y, Iikura Y. Altered eosinophil levels as a result of viral infection in asthma exacerbation in childhood. *Pediatr Allergy Immunol* 2002;13:47–50.
35. Sampath D, Castro M, Look DC, Holtzman MJ. Constitutive activation of an epithelial signal transducer and activator of transcription (STAT) pathway in asthma. *J Clin Invest* 1999;103:1353–1361.
36. Walter MJ, Morton JD, Kajiwara N, Agapov E, Holtzman MJ. Viral induction of a chronic asthma phenotype and genetic segregation from the acute response. *J Clin Invest* 2002;110:165–175.